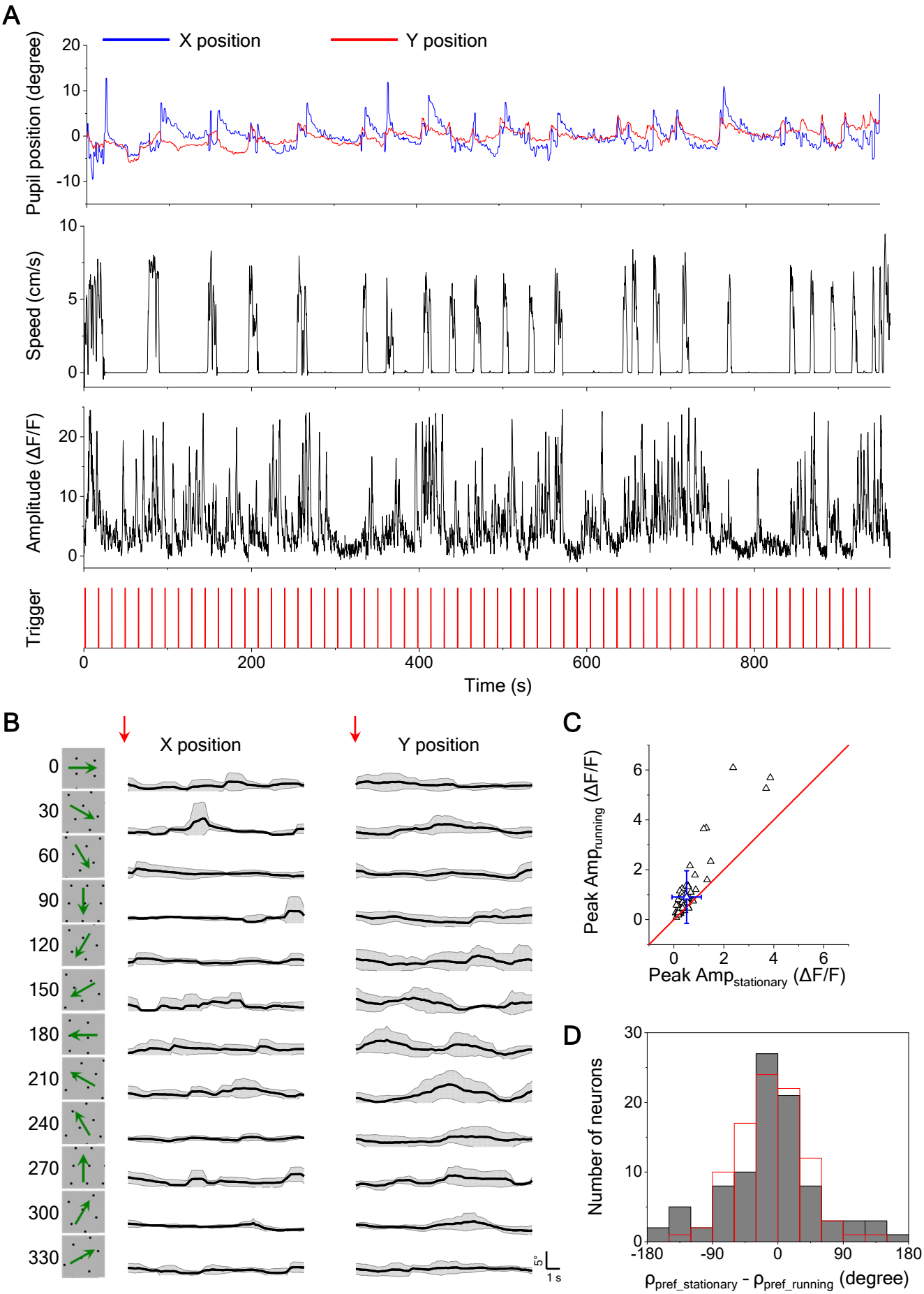
A
X position
Y position
Pupil position (degree)
Speed (cm/s)
Amplitude (ΔF/F)
Trigger
Time (s)
B
X position
Y position
0
30
60
90
120
150
180
210
240
270
300
330
5°
1 s
C
Peak Amp running (ΔF/F)
Peak Amp stationary (ΔF/F)
D
Number of neurons
ρpref_stationary - ρpref_running (degree)

Figure S1. Effects of Behavioral States on Visual Responses. Related to Figure 1.

(A) An example showing pupil position, running speed, and calcium responses of a single neuron to moving dots stimuli.

(B) Traces of pupil position averaged over identical stimulus trials for each direction of motion. Red arrow indicates the stimulus onset. Gray shade indicates the standard deviation across identical trials.

(C) Peak amplitude of calcium responses to moving dots in 12 directions in the running state versus that in the stationary state (n = 93 cells).

(D) Histogram of the difference between preferred direction in the stationary state and that in the running state (-11°±65°, n = 93 cells). Note the distribution is similar to a control histogram from comparing two sets of stationary trials (unfilled red bars, -10°±47°).

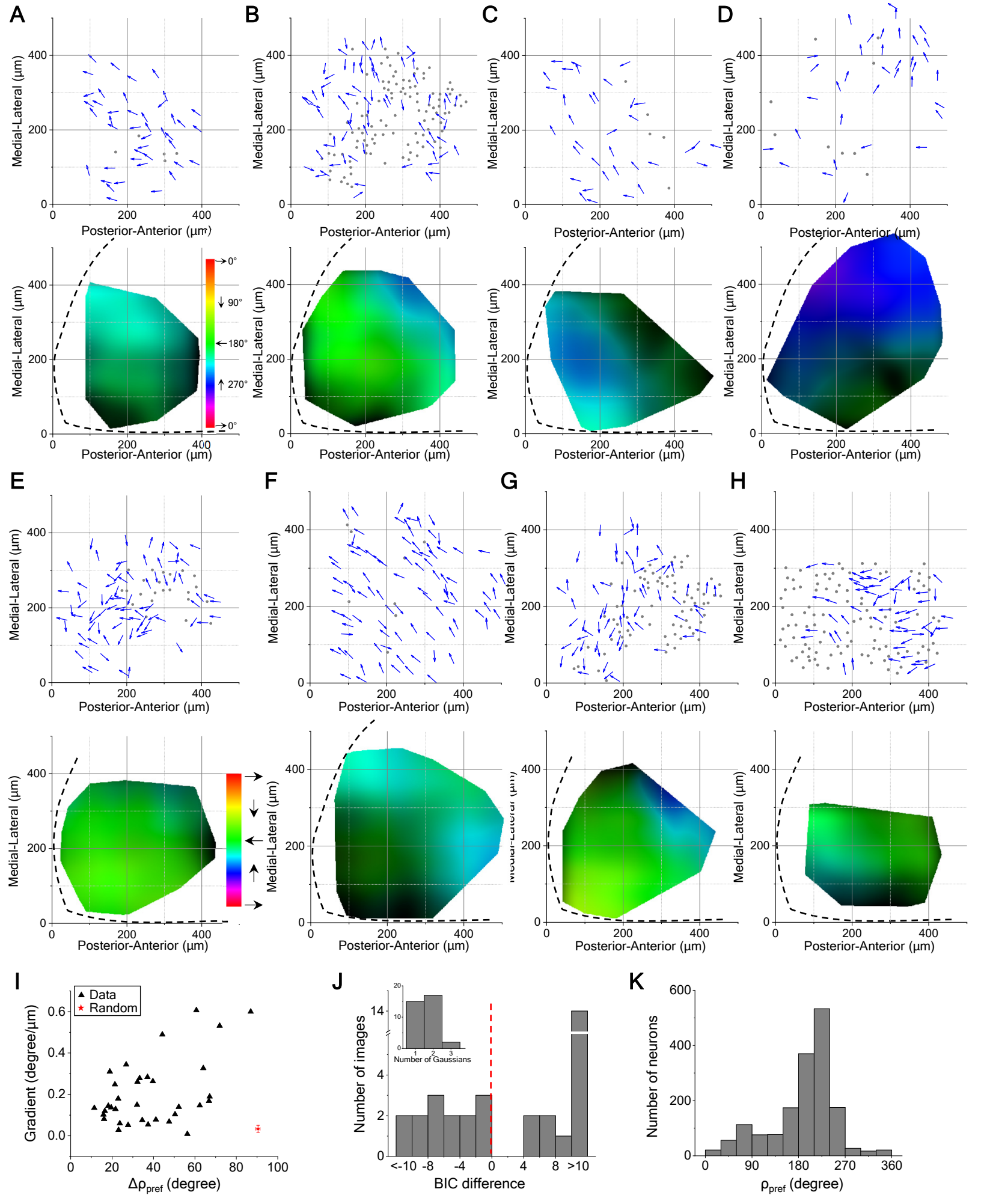
A
B
C
D
E
F
G
H
I
J
K
Medial-Lateral (μm)
Posterior-Anterior (μm)
0°
90°
180°
270°
0°
Data
Random
Gradient (degree/μm)
Δρpref (degree)
Number of images
Number of Gaussians
BIC difference
<-10
-8
-4
0
4
8
>10
Number of neurons
ρpref (degree)

Figure S2. Organization of Motion Direction Measured by Moving Dots and Moving Bars. Related to Figure 2.

(A, B, C, D) Data from 4 animals stimulated with moving dots, presented as in Figures 2A and 2C.

(E, F, G, H) Data from 4 animals stimulated with moving bars, presented as in Figures 2A and 2C.

(I) Gradients of the map plotted against the absolute difference in preferred directions for pairs within 50 μm (33 images) measured with moving bars, displayed as in Figure 2M.

(J) Analysis of bimodality in the distributions of preferred direction (33 images) measured with moving bars, displayed as in Figure 2N.

(K) Histograms of preferred direction for all direction-selective neurons (1660 cells) measured with moving bars.

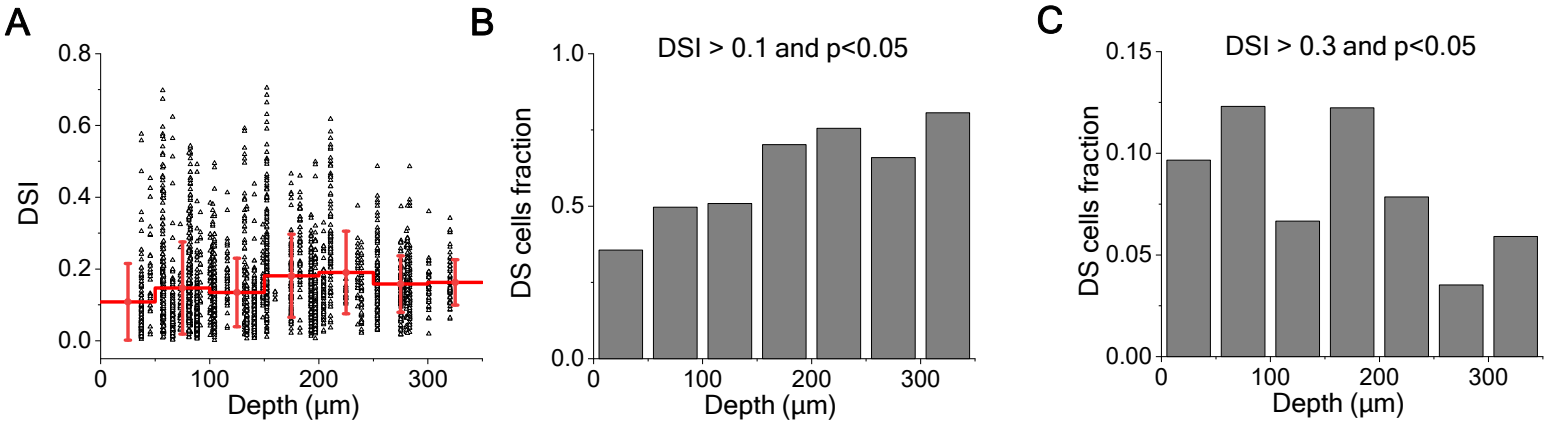
A
B
C
DSI
0.8
0.6
0.4
0.2
0.0
0
100
200
300
Depth (µm)
DS cells fraction
DSI > 0.1 and p<0.05
1.0
0.5
0.0
DSI > 0.3 and p<0.05
0.15
0.10
0.05
0.00

Figure S3. Direction Selectivity as a Function of Depth in the SC. Related to Figure 3.

(A) DSI of each neuron as a function of depth in the SC. Red line indicates the mean and the standard deviation.

(B) Fraction of DS cells as a function of depth.

(C) Fraction of cells with high DSI as a function of depth.

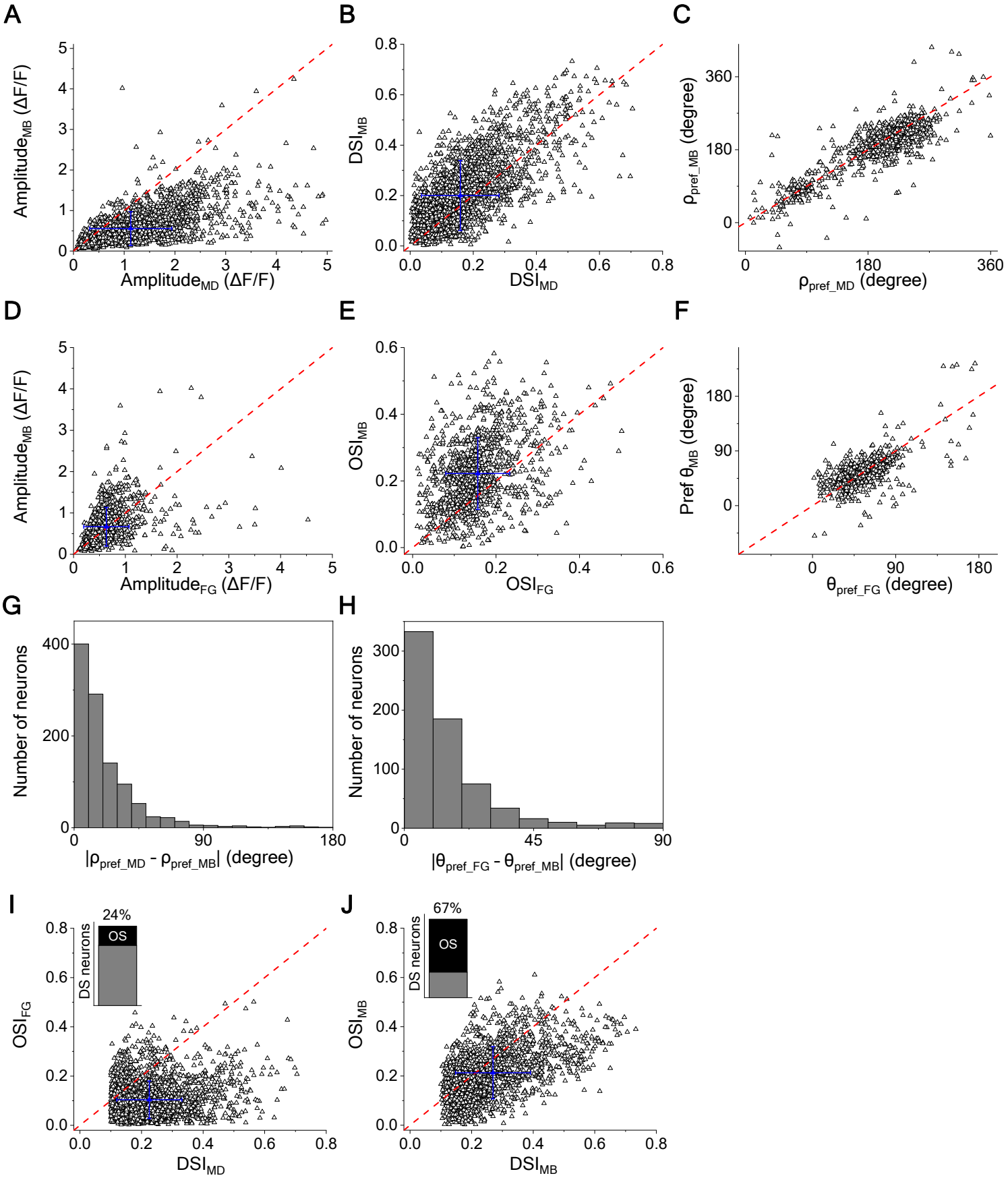
A
Amplitude$_{MB}$ (ΔF/F)
Amplitude$_{MD}$ (ΔF/F)
B
DSI$_{MB}$
DSI$_{MD}$
C
ρ$_{pref_MB}$ (degree)
ρ$_{pref_MD}$ (degree)
D
Amplitude$_{MB}$ (ΔF/F)
Amplitude$_{FG}$ (ΔF/F)
E
OSI$_{MB}$
OSI$_{FG}$
F
Pref θ$_{MB}$ (degree)
θ$_{pref_FG}$ (degree)
G
Number of neurons
|ρ$_{pref_MD}$ - ρ$_{pref_MB}$| (degree)
H
Number of neurons
|θ$_{pref_FG}$ - θ$_{pref_MB}$| (degree)
I
24%
OS
DS neurons
OSI$_{FG}$
DSI$_{MD}$
J
67%
OS
DS neurons
OSI$_{MB}$
DSI$_{MB}$

Figure S4. Motion Direction and Orientation Measured by Different Visual Stimuli. Related to Figure 4.

(A) Response amplitude to moving bars plotted against that to moving dots (2351 neurons from 14 animals) .

(B) DSI measured by moving bars plotted against that by moving dots (2351 neurons from 14 animals).

(C) Preferred direction measured by moving bars plotted against that by moving dots for DS neurons (1071 neurons from 14 animals).

(D) Response amplitude to moving bars plotted against that to flashed gratings (1081 neurons from 14 animals).

(E) OSI measured by moving bars plotted against that by flashed gratings (1081 neurons from 14 animals).

(F) Preferred orientation measured by moving bars plotted against that by flashed gratings for DS neurons (675 neurons from 14 animals).

(G) Histogram of difference between preferred directions measured by moving dots and moving bars (1071 neurons from 14 animals).

(H) Histogram of difference between preferred orientations measured by flashed gratings and moving bars (675 neurons from 14 animals).

(I) OSI measured by flashed gratings plotted against DSI by moving dots for DS neurons (2187 neurons from 14 animals). Inset, percentage of OS-DS neurons in DS neurons.

(J) OSI plotted against DSI measured by moving bars for DS neurons (1693 neurons from 14 animals). Inset, percentage of OS-DS neurons in DS neurons.

A

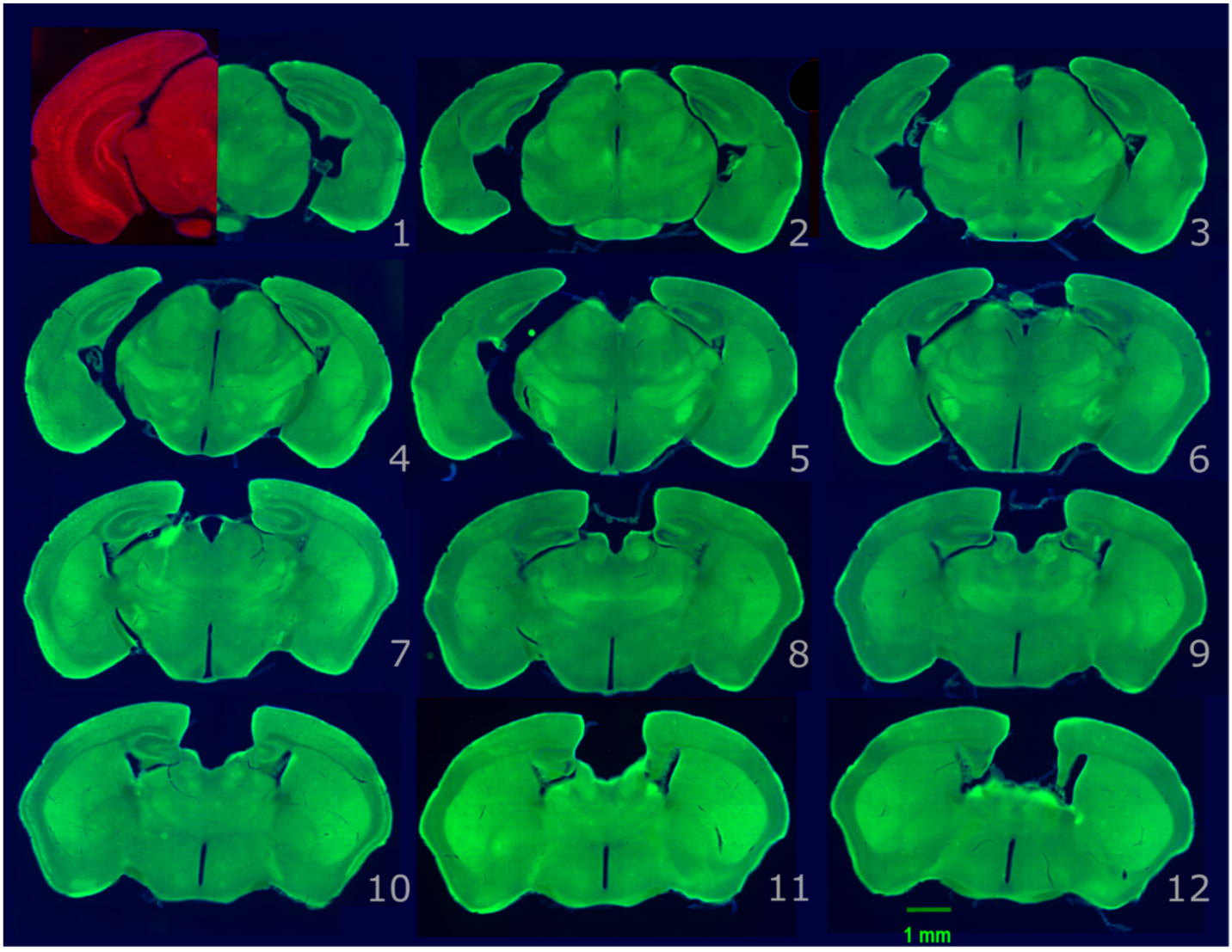
1
2
3
4
5
6
7
8
9
10
11
12
1 mm

B

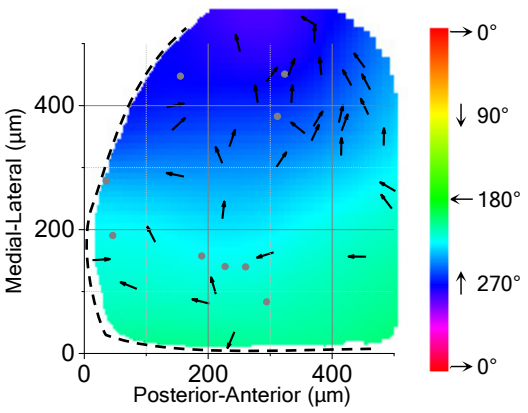
Medial-Lateral (μm)
400
200
0
0
200
400
Posterior-Anterior (μm)
0°
90°
180°
270°
0°

C

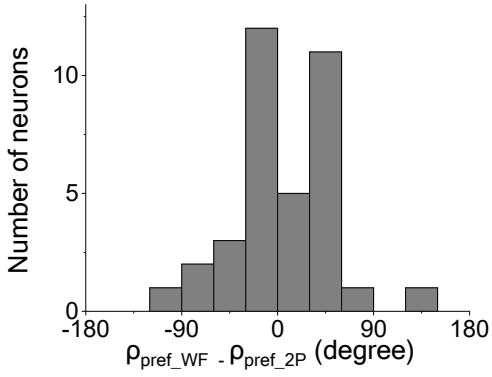
Number of neurons
10
5
0
-180
-90
0
90
180
ρpref_WF - ρpref_2P (degree)

Figure S5. Validate the Approach of Imaging the Entire Superior Colliculus of Partial-Cortex Mutant Mice Using a Wide-Field Imaging Technique. Related to Figure 5.

(A) Brain Anatomy of a Mutant Mouse (Emx1-cre:pals1$^{flox/Wt}$) with Partially Developed Neocortex. Series of coronal sections (100 μm thick) labeled from anterior (1) to posterior (12). The left half of panel 1 shows the corresponding section from a wild-type mouse brain. Color indicates autofluorescence.

(B) Overlay of arrow plots from 2-photon imaging data and direction map from wide-field imaging data. Hue encodes the preferred direction.

(C) Histogram of difference of preferred directions for the data in (B).

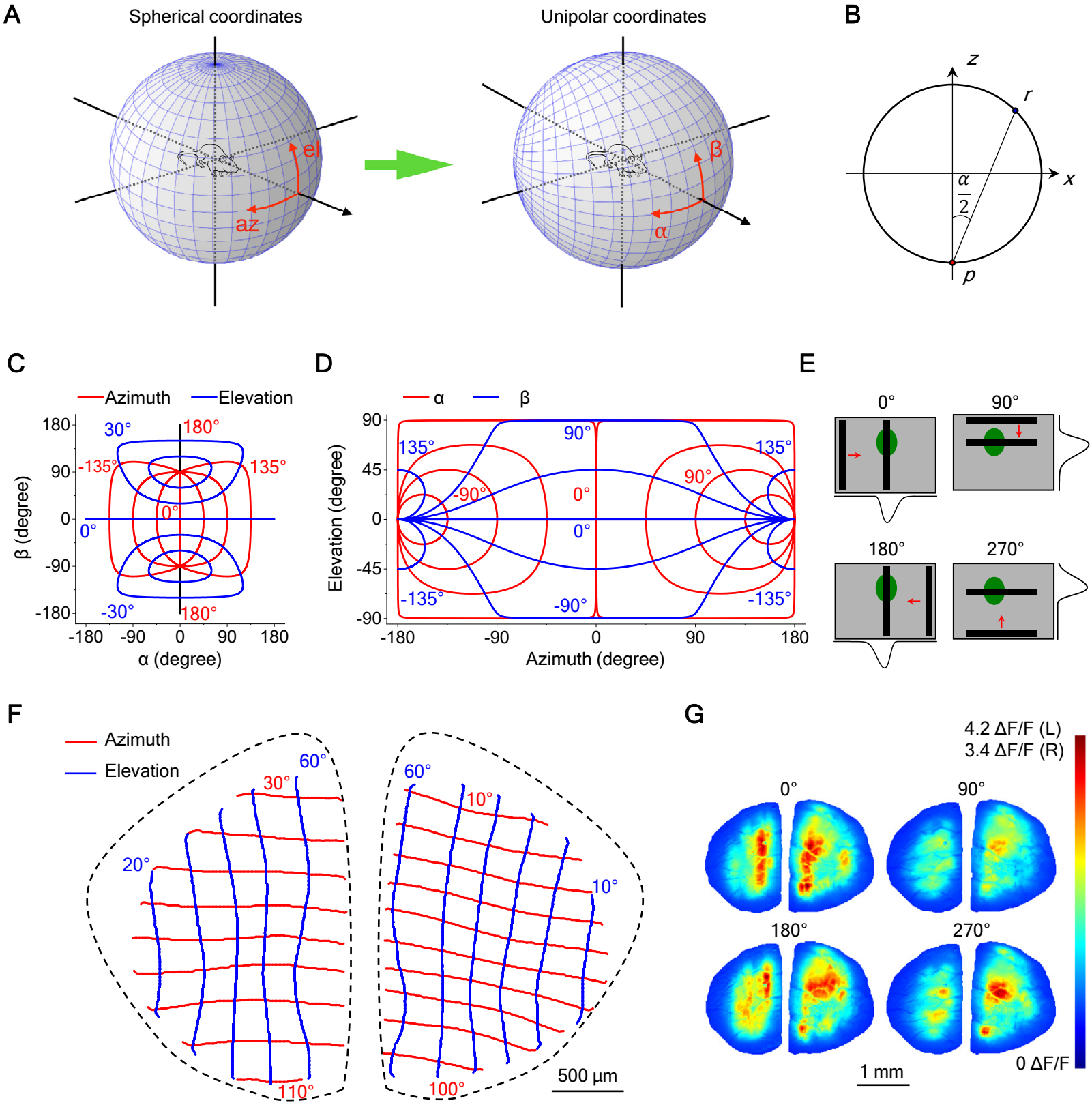
A
Spherical coordinates
Unipolar coordinates
el
az
β
α
B
z
r
x
α/2
p
C
Azimuth
Elevation
β (degree)
α (degree)
D
α
β
Elevation (degree)
Azimuth (degree)
E
0°
90°
180°
270°
F
Azimuth
Elevation
500 μm
G
4.2 ΔF/F (L)
3.4 ΔF/F (R)
0 ΔF/F
1 mm

Figure S6. Large-Scale Direction Maps in Visual Space With Unipolar Coordinates and Anatomical Space. Related to Figure 6.

(A) Schematic illustrating the correspondence of spherical coordinates and unipolar coordinates.

(B) Schematic defining the unipolar coordinates (see STAR METHODS).

(C) and (D) Relationship between spherical coordinates and unipolar coordinates.

(E) Schematic illustrating how the RF location is derived from the time course of the response to moving bars.

(F) Visuotopic map of both sides of superior colliculus of a partial cortex mutant mouse derived from receptive field measurements with moving bars.

(G) Peak amplitudes of trial-averaged calcium responses to moving dots at four directions for both sides of superior colliculus of a partial cortex mutant mouse.

Figure S7. Related to Figure 7

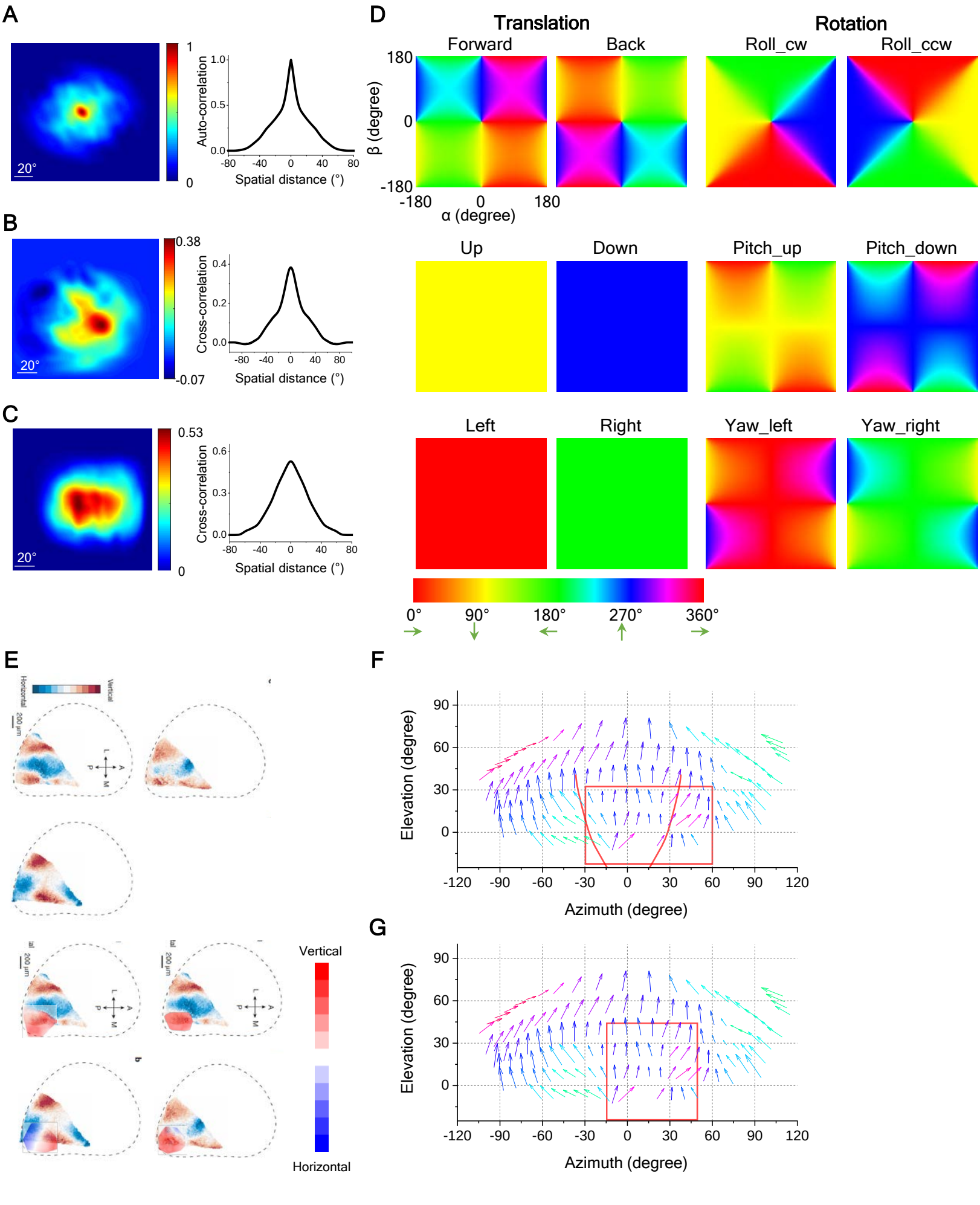

Figure S7. Quantify the Patch Size and Behavioral Relevance of Global Direction Maps and Relation to Prior Work. Related to Figure 7.

(A) Left, the autocorrelation of a sample direction map. Right, the corresponding radial profile.

(B) Left, the cross-correlation between direction maps of the left and right SCs of an example animal. Right, the corresponding radial profile, centered on the peak of the correlation map.

(C) Left, the cross-correlation between direction maps of the same-side SCs of two different animals. Right, the corresponding radial profile.

(D) For each of the 6 basic modes of translation and rotation, this plots the direction of the optic flow vectors in the visual field using unipolar coordinates. Note these graphs assume that the axis of forward translation and roll rotation equals the lambda-bregma axis. In actuality, a freely moving mouse may carry the head inclined downward during ambulation [S1] or upward during rearing.

(E) Orientation maps predicted from direction maps according to their orthogonal relationship and overlaid with Figure 4 in [S2].

(F) Arrow plots of the preferred direction in the SC, averaged over 9 animals, and plotted across the visual field in spherical coordinates. The red rectangle indicates the overlapping visual space with Figure 3E in [S3]. The red curves indicate the monocular-binocular border.

(G) The same plot as (F). The red rectangle indicates the overlapping visual space with Figure 4h in [S4].

SUPPLEMENTAL REFERENCES

S1.Oommen, B.S., and Stahl, J.S. (2008). Eye orientation during static tilts and its relationship to spontaneous head pitch in the laboratory mouse. Brain Research 1193, 57–66.

S2.Feinberg, E.H., and Meister, M. (2015). Orientation columns in the mouse superior colliculus. Nature 519, 229–232.

S3de Malmazet, D., Kühn, N.K., and Farrow, K. (2018). Retinotopic Separation of Nasal and Temporal Motion Selectivity in the Mouse Superior Colliculus. Current Biology 28, 2961-2969.e4.

S4Ahmadlou, M., and Heimel, J.A. (2015). Preference for concentric orientations in the mouse superior colliculus. Nat Commun 6, 6773.